

See discussions, stats, and author profiles for this publication at: <https://www.researchgate.net/publication/283356024>

Study and Development of Parallel Robots Based On 5-Bar Linkage

Conference Paper · October 2015

CITATIONS

3

READS

8,083

3 authors, including:



[Tuong Manh Hoang](#)

Ho Chi Minh City University of Technology

1 PUBLICATION 3 CITATIONS

[SEE PROFILE](#)



[Cong Bang Pham](#)

Ho Chi Minh City University of Technology

26 PUBLICATIONS 684 CITATIONS

[SEE PROFILE](#)

STUDY AND DEVELOPMENT OF PARALLEL ROBOTS BASED ON 5-BAR LINKAGE

Manh Tuong Hoang, Trung Tin Vuong, Cong Bang Pham

Department of Mechatronic Engineering, Faculty of Mechanical Engineering, Ho Chi Minh City University of Technology – Viet Nam

Email: {41104135, 21103658, cbpham}@hcmut.edu.vn

ABSTRACT

Nowadays, parallel robots are used popularly in industry because of its flexibility, high rigidity and high loading capacity. However, in contrast of those benefits, they still exist main drawbacks as small workspace interrupted by singularity zones. This paper attempts to study how a parallel robot based on 5-bar linkage works. Major issues include conceiving a 5-bar linkage, designing a 2-DOF parallel robot through workspace synthesis, singularity analysis and structure design, implementing a prototype and control system. System operation as well as experimental results validate this approach.

Keywords: Parallel robot, 5-bar linkage, workspace synthesis

1. INTRODUCTION

Thanks to the development of technology, the robot was invented to release humans from heavy, dangerous and toxic work. The most common applications of robots in industry can be listed as painting, welding, assembling, etc. Along with the development of technology applying in industrial robots, a concept of computer numerical control (CNC) was invented to meet higher accuracy, automation, and flexibility of production. Since its invention in the 40s of the 20th century, CNC machines are expanded their application on various fields. Beside multi-axis machines used in manufacturing, 2-axis CNC systems are still found useful in many applications as shown in Fig. 1a (decoration) and Fig. 1b (2-D boundary cutting). With a variety in cutting tools, they are also commonly used in laser cutting technology, plasma cutting, welding, etc.



a) Pattern engraving



b) 3D product

Figure 1. Products from 2-D CNC systems

Conventional 2-DOF CNC systems commonly use the ball screw/nut mechanism. They look like a conventional serial manipulator in which links are connected in series through joints. The advantages of a serial mechanism are its large workspace and high dexterity. However, because of its cantilever-like structure, a serial mechanism has large moving mass, low stiffness and low loading capacity. Pham [1] has proposed a novel design of a 2-dimensional CNC system in which only a timing belt is used to conduct motions in X and Y directions. Its advantages are that the design is simple, light weight and easy to expand its workspace as shown in Fig. 2. This system is an example of parallel manipulators in which the end-effector is connected to the base through several serial kinematic chains or 'legs'. Because of the elastic property of the timing belt, this system has some limitations in rigidity and loading capacity.

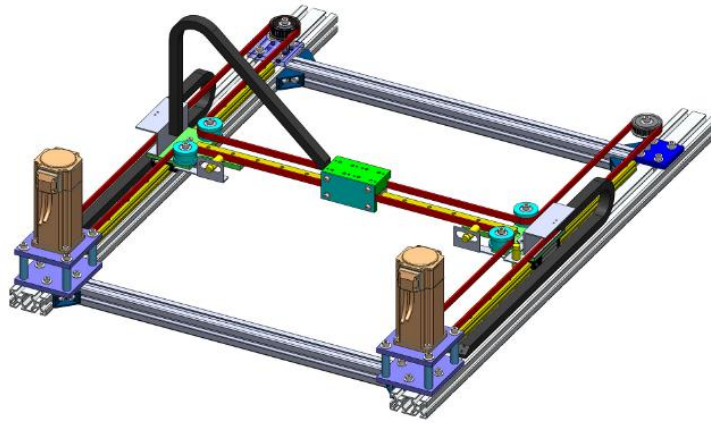


Figure 2. Belt-driven 2-D CNC Systems

In this paper, a 2-DOF parallel robot composed of rigid links and joints is studied and developed. It has a structure of 5-bar linkage and therefore possesses advantages of low moment of inertia, high rigidity and high loading capacity. The organization of this paper is as follows: Section 2 presents kinematic analyses of the 2 DOF parallel robot. This is followed by workspace and singularity analysis in Section 3. Criteria of mechanical design are presented in Section 4. Section 5 addresses electrical components as well as connection diagrams. Control algorithms along with experimental results are discussed in Section 6. The paper is concluded in Section 7.

2. KINEMATIC ANALYSIS

Kinematic analysis is necessary to build the mathematical model of the robot. The aim is to establish the relation between joint angles and the coordinates of the end-effector. The 5-bar parallel robot with revolute joints and symmetric design is considered. The length of the links and the fixed joints coordinates are shown in Fig. 3.

Two actuators are located at O and B, having rotation angles denoted by θ_1 and θ_4 , respectively. The end-effector is fixed at P. From Fig. 3, the following vector equation can be derived:

$$\begin{aligned} \overrightarrow{OP} &= \overrightarrow{OA} + \overrightarrow{AP} = \overrightarrow{OB} + \overrightarrow{BC} + \overrightarrow{CP} \\ \Leftrightarrow \begin{Bmatrix} x_P \\ y_P \end{Bmatrix} &= \begin{Bmatrix} l_a \cos \theta_1 + l_b \cos \theta_2 \\ l_a \sin \theta_1 + l_b \sin \theta_2 \end{Bmatrix} = \begin{Bmatrix} l_c + l_a \cos \theta_4 + l_b \cos \theta_3 \\ l_a \sin \theta_4 + l_b \sin \theta_3 \end{Bmatrix} \end{aligned} \quad (1)$$

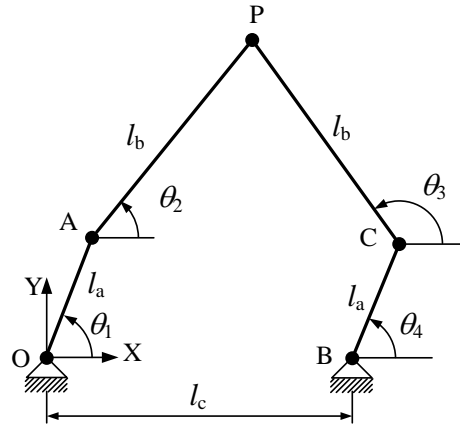


Figure 3. Schematic of five-bar linkage

2.1 Forward Kinematic

Given the joint angles (θ_1, θ_4) , eliminating terms θ_2 and θ_3 in Eqn. (1) leads to the coordinates of end-effector at P as follows:

$$\begin{cases} x_P = l_c + l_a \cos \theta_4 + l_b \cos \left[2 \arctan \left(\frac{-F \pm \sqrt{E^2 + F^2 - G^2}}{G - E} \right) \right] \\ y_P = l_a \sin \theta_4 + l_b \sin \left[2 \arctan \left(\frac{-F \pm \sqrt{E^2 + F^2 - G^2}}{G - E} \right) \right] \end{cases} \quad (2)$$

Where

$$E = 2l_b (l_c + l_a (\cos \theta_4 - \cos \theta_1))$$

$$F = 2l_a l_b (\sin \theta_4 - \sin \theta_1)$$

$$G = l_c^2 + 2l_a^2 + 2l_c l_a \cos \theta_4 - 2l_c l_a \cos \theta_1 - 2l_a^2 \cos(\theta_4 - \theta_1)$$

When solutions exist in Eqns. (2), one input results in two sets of end-effector coordinates. Their configurations are demonstrated in Fig. 4.

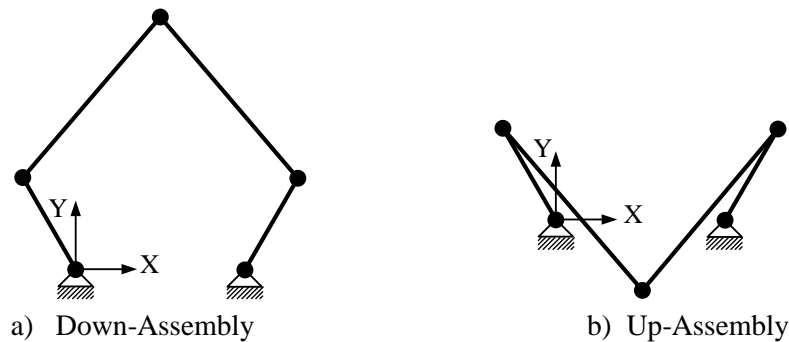


Figure 4. Two configurations in the forward kinematic problem

2.2 Inverse Kinematic

Knowing the coordinates of the end-effector at point P (x_P , y_P), the rotation angles of actuators can be calculated in Eqns (3).

$$\begin{cases} \theta_1 = 2 \arctan \left(\frac{-F_1 \pm \sqrt{E_1^2 + F_1^2 - G_1^2}}{G_1 - E_1} \right) \\ \theta_4 = 2 \arctan \left(\frac{-F_4 \pm \sqrt{E_4^2 + F_4^2 - G_4^2}}{G_4 - E_4} \right) \end{cases} \quad (3)$$

Where

$$\begin{aligned} E_1 &= -2l_a x_P & E_4 &= 2l_a (-x_P + l_c) \\ F_1 &= -2l_a y_P & F_4 &= -2l_a y_P \\ G_1 &= l_a^2 - l_b^2 + x_P^2 + y_P^2 & G_4 &= l_c^2 + l_a^2 - l_b^2 + x_P^2 + y_P^2 - 2l_c x_P \end{aligned}$$

It can be seen in Eqns. (3) that there are always four solutions in the inverse kinematic problem within the workspace. Combination of the '+' sign and '-' of θ_1 and θ_4 leads to four configurations of the robot as demonstrated in Fig. 5.

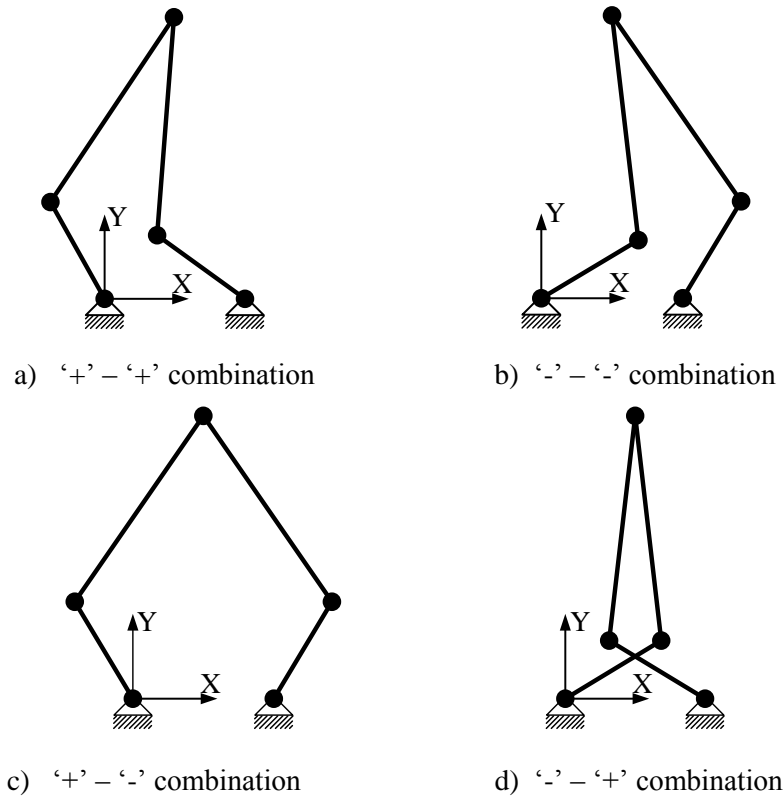


Figure 5. Four configurations in the forward kinematic problem

3. WORKSPACE AND SINGULARITY ANALYSIS

3.1 Workspace analysis

A workspace is defined as the region that the end-effector of the robot can reach when the joint angles θ_1 and θ_4 fully rotate. Analyzing the workspace is an essential problem in designing robot, particularly in determining link lengths to satisfy some given working areas.

This parallel robot is decomposed into two 2-DOF serial mechanisms. With the length of l_a , l_b is given, each serial chain creates a working area having a doughnut shape limited by two circle boundaries as seen in Fig. 6. Therefore, the workspace of the 2-DOF parallel robot is an intersection of these two working areas as illustrated in Fig. 7.

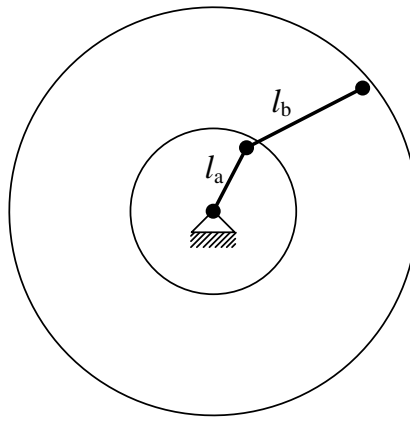


Figure 6. Workspace generated by the 2-DOF serial chains

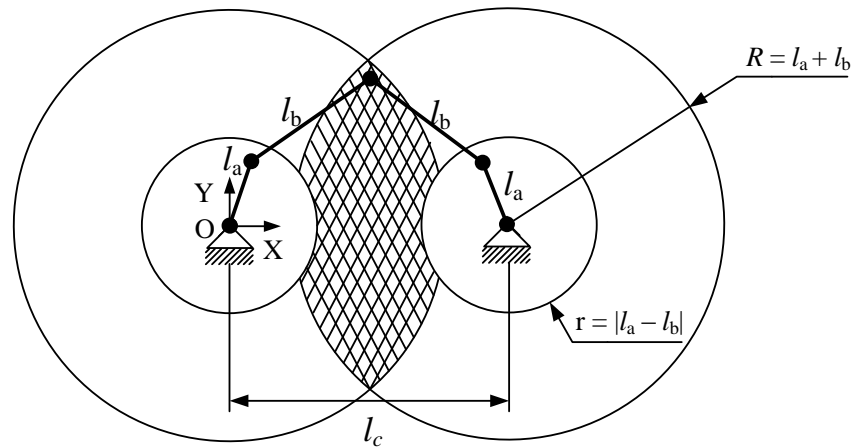
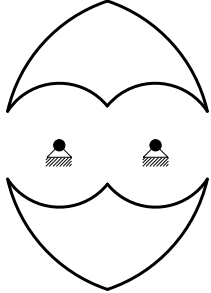
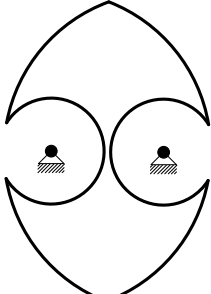
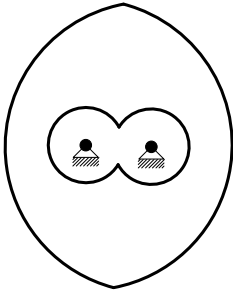
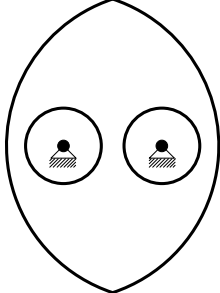
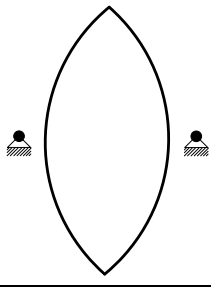


Figure 7. Workspace of 2-DOF parallel robot

Depending on the relation between the link lengths (l_a , l_b , l_c), Table 1 lists five various types of workspace. Due to symmetric design, it can be realized that these workspaces are symmetric about the x-axis and about the vertical line $x = l_c/2$.

Table 1: Five types of workspace shapes for the 2-DOF parallel robot

Type	Shape	Condition
1		$\begin{cases} l_c - r < R < l_c + r \\ r > \frac{l_c}{2} \end{cases} \Leftrightarrow \begin{cases} 2l_a < l_c < 2l_b \\ l_b > \frac{l_c}{2} + l_a \end{cases} (l_b > l_a)$
2		$\begin{cases} l_c - r < R < l_c + r \\ r \leq \frac{l_c}{2} \end{cases} \Leftrightarrow \begin{cases} 2l_a < l_c < 2l_b \\ l_b \leq \frac{l_c}{2} + l_a \end{cases} (l_b > l_a)$
3		$\begin{cases} R \geq l_c + r \\ r > \frac{l_c}{2} \end{cases} \Leftrightarrow \begin{cases} l_c \leq 2l_a \\ l_b > \frac{l_c}{2} + l_a \end{cases} (l_b > l_a)$
4		$\begin{cases} R \geq l_c + r \\ r \leq \frac{l_c}{2} \end{cases} \Leftrightarrow \begin{cases} l_c \leq 2l_a \\ l_b \leq \frac{l_c}{2} + l_a \end{cases} (l_b > l_a)$
5		$\begin{cases} \frac{l_c}{2} \leq R \leq l_c - r \\ r > \frac{l_c}{2} \end{cases} \Leftrightarrow \begin{cases} 2l_b \leq l_c \leq 2l_a + 2l_b \\ l_b > \frac{l_c}{2} + l_a \end{cases} (l_b > l_a)$

3.2 Singularity analysis

In comparison with serial robots, a parallel robot have many advantages such as: high rigidity, accuracy, speed, and high payload. However, the kinematic analysis problem is more complicated, and during the operation of the parallel robot, the existing of singularity regions are frequently causes of the non-operational. Therefore, singularity analysis is extremely important to overcome this problem. Singularity is analyzed from the relationship between velocity of the joint angles $\dot{\theta}$ and velocity of the end-effector \dot{x} which can be expressed as:

$$A\dot{x} + B\dot{\theta} = 0$$

Where A and B are both 2×2 Jacobian matrices, depending on the current posture of the robot.

In the left chain OAP of the robot in Fig. 3, the linear velocity of the end-effector can be derived from the angular velocity of OA (ω_1) and the angular velocity of AP (ω_2) as follows:

$$\mathbf{v}_P = \omega_1 \times \overline{OA} + \omega_2 \times \overline{AP} \quad (4)$$

Multiplying \overline{AP} to the two sides of Eqn. (4) leads to

$$l_b \cdot \cos(\theta_2) \cdot v_{Px} + l_b \cdot \sin(\theta_2) \cdot v_{Py} = \dot{\theta}_1 \cdot l_a \cdot l_b \cdot \sin(\theta_2 - \theta_1) \quad (5)$$

Do similarly to the right chain BCP, the linear velocity of the end-effector can be determined from the joint angle velocity $\dot{\theta}_4$ as follows:

$$l_b \cdot \cos(\theta_3) \cdot v_{Px} + l_b \cdot \sin(\theta_3) \cdot v_{Py} = \dot{\theta}_4 \cdot l_a \cdot l_b \cdot \sin(\theta_3 - \theta_4) \quad (6)$$

Combining Eqns. (5) and (6) leads to

$$\mathbf{A} \cdot \begin{bmatrix} v_{Px} \\ v_{Py} \end{bmatrix} = \mathbf{B} \cdot \begin{bmatrix} \dot{\theta}_1 \\ \dot{\theta}_4 \end{bmatrix} \quad (7)$$

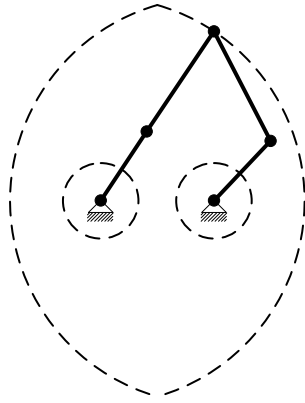
$$\text{Where } \mathbf{A} = \begin{bmatrix} l_b \cdot \cos(\theta_2) & l_b \cdot \sin(\theta_2) \\ l_b \cdot \cos(\theta_3) & l_b \cdot \sin(\theta_3) \end{bmatrix}, \quad \mathbf{B} = \begin{bmatrix} l_a \cdot l_b \cdot \sin(\theta_2 - \theta_1) & 0 \\ 0 & l_a \cdot l_b \cdot \sin(\theta_3 - \theta_4) \end{bmatrix}$$

Depending on the invertibility of \mathbf{A} and \mathbf{B} , the singularity of the robot can be classified into three types [2]: type I (when $\det(\mathbf{B}) = 0$), type II (when $\det(\mathbf{A}) = 0$) and type III (when $\det(\mathbf{A}) = \det(\mathbf{B}) = 0$) as shown in Fig. 8.

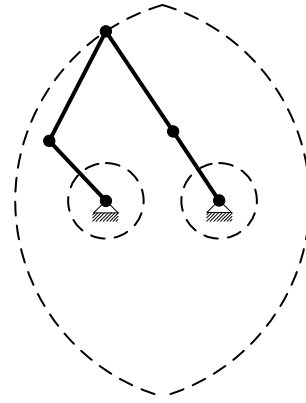
The type I singularity occurs when: $\sin(\theta_2 - \theta_1) \cdot \sin(\theta_3 - \theta_4) = 0$. It can be realized that this type corresponds to configurations in which the chains extend (Fig. 8a) or fold (Fig. 8b) completely. Therefore, the collection of type I singularity points is on the workspace boundaries.

The type II singularity brings about: $\sin(\theta_3 - \theta_2) = 0$. This type corresponds to configurations in which two passive links are in alignment as seen in Fig. 8c. The collection of type II singularity points are some areas within the workspace.

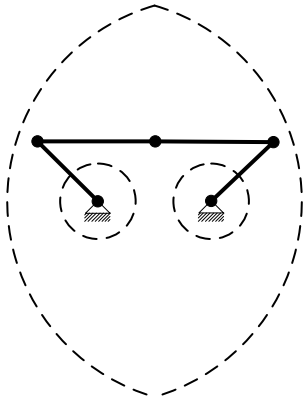
The type III singularity is a special case, referring to architecture singularity where five points O, A, P, C and B are collinear shown as in Fig. 8d.



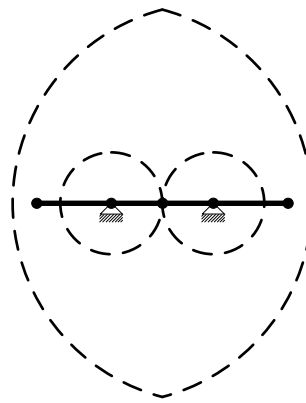
a) The left chain extend completely



b) The right chain fold completely



c) Two passive links are in alignment



d) The links are collinear

Figure 8. Some configurations corresponding to the singularities

4. MECHANICAL DESIGN

The process design for the 2-DOF parallel robot consists of determining link parameters and actuator powers to achieve desired performance. In details, there are four design criteria as follows:

Design criteria 1: Avoiding the interference between the two active links.

As shown in Fig. 9, in order to fully rotate without colliding, the length of two active links is constrained as follows:

$$l_c = 2.l_a + k \quad (8)$$

Where k is a safety distance (> 0).

Following the workspace analysis in Table 1, there are only workspaces of type 1, type 2 and type 5 existing with the constraint in Eqn. (8).

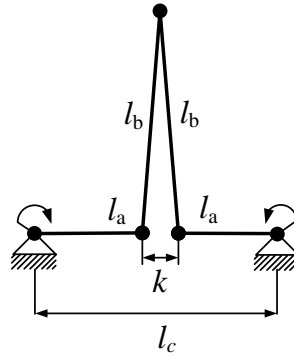


Figure 9. Two active links fully rotate

Design criteria 2: Eliminating the type II and type III singularity

As discussed in Section 3.2, the type I singularity always exists and occurs in workspace boundaries. However, the type II and type III singularities can be eliminated with proper values of the link length. This can be achieved from the followings:

$$\begin{cases} l_c > 2l_a & (\text{two passive links cannot be completely folded}) \\ l_b > \frac{l_c}{2} + l_a & (\text{two passive links cannot be completely stretched}) \end{cases} \quad (9)$$

As a result from Eqn. (9), there is only type 1 workspace left.

Design criteria 3: The workspace encloses a rectangle of $l_w \times h_w$.

Figure 10 shows a typical workspace covering the desired rectangle in which four vertexes are on the four segments of the workspace boundaries. To make this happen, the following conditions have to be satisfied:

$$\sqrt{R^2 - \left(\frac{l_c + l_w}{2}\right)^2} - \sqrt{r^2 - \left(\frac{l_c - l_w}{2}\right)^2} = h_w \quad (10)$$

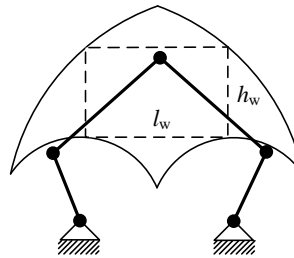


Figure 10. A typical workspace covering the desired rectangle

Combining Eqns. (8) (9) and (10) gives multiple solutions of the link lengths. In this design, the rectangle has dimensions of 110 mm \times 90 mm, and the link lengths are calculated and chosen as $l_a = 70$ mm, $l_b = 200$ mm, and $l_c = 250$ mm.

Design criteria 4: Sustaining a 1 kg payload and speeding up to 2 m/s over 1 second.

The links have to be stiff enough to sustain 1 kg payload. In this study, Solidworks Simulation tool is utilized to determine rectangular cross-section of the links. Table 2 shows the dimension results as well as the material of the links.

Table 2: Link Parameters

Link	l_a	l_b	l_c
Length	70 mm	200 mm	250 mm
Cross-section	10 mm \times 30 mm	10 mm \times 30 mm	\times
Mass	90 g	195 g	\times
Material	Aluminum	Aluminum	\times

From the link parameters above and the desired performance of the end-effector, the necessary moment and the power of the motor are 0.59 N.m and 12 W, respectively. Two AC servo motors Mitsubishi HC-KFS23 are employed with their specifications as shown in Table 3.

Table 3: Main specifications of motor

Power Rated output (W)	200
Rated Input Voltage (VAC)	200-230 (50/60 Hz)
Rated current (A)	1.1
Rated torque (N.m)	0.64
Rated speed (r/min)	3000
Encoder resolution (p/rev)	131072

Through Section 3, a 3D model of the 2-DOF parallel robot in SolidWorks is illustrated in Fig. 11. There are three main components: block of base plate, block of motor and link system.

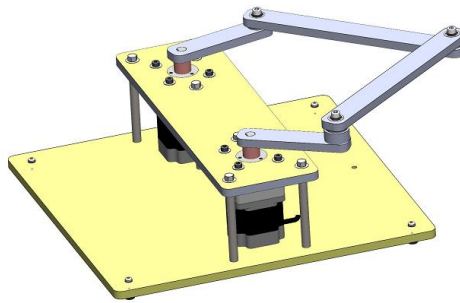


Figure 11. 3D model of the 2-DOF parallel robot

5. ELECTRICAL DIAGRAM

Figure 12 shows components of the 2-DOF parallel robot. Two AC servo motors are controlled by two drivers MR-J2S-20A. The drivers have three operational modes: position control, speed control and torque control. During operating, these three modes can be switched together. A multi-

axis motion controller card is need to command the drivers and control two motors synchronously. In this system, a PISO-PS400 is employed as a controller. The card plugged into the PCI port of the computer has 100 output pins to communicate with peripheral devices. The card can control simultaneously 4-axis stepping/pulse-type servo motor. It can capture the pulses of encoder with high speed 500000 PPS and store position with high range $\pm 2^{31}$ pulses per axis. Being supported with libraries in C#, it's useful to build applications with complex movements.

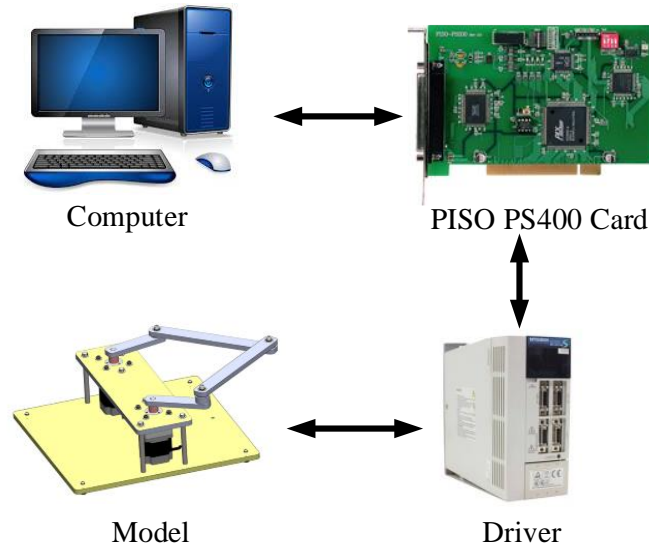


Figure 12. Control system diagram

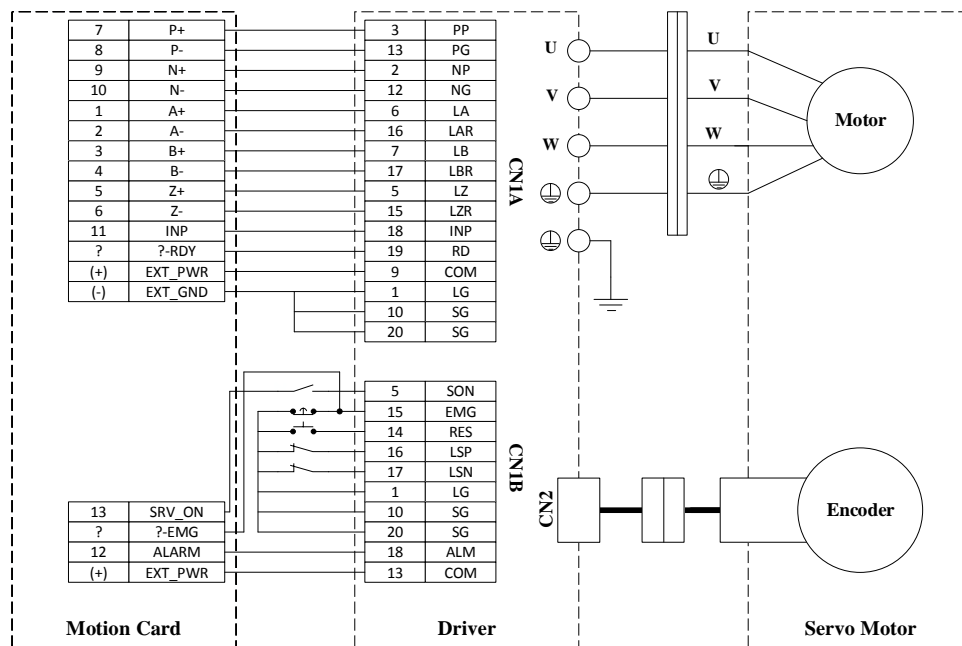


Figure 13. Card-Driver connection diagram

The connection diagram between the card and the drivers is demonstrated in Fig. 13. In this case,

the position control mode of the drivers is set. Forward/reverse rotation pulse trains are transferred from the motion controller card to the drivers that makes the servo motors move. Motor position is fed back into the drivers through CN2 port. These signals are also transmitted backward to the motion controller card for synchronization. Between the motion card and the drivers, there are also triggered signals such as Emergency, Driver Enable and Error Alarm.

6. CONTROL SYSTEM IMPLEMENTATION

6.1 Interpolation algorithm

A motion profile is usually interpolated into linear and circular elements. Therefore, control algorithm of linear motion and circular motion is essential to create certain movement.

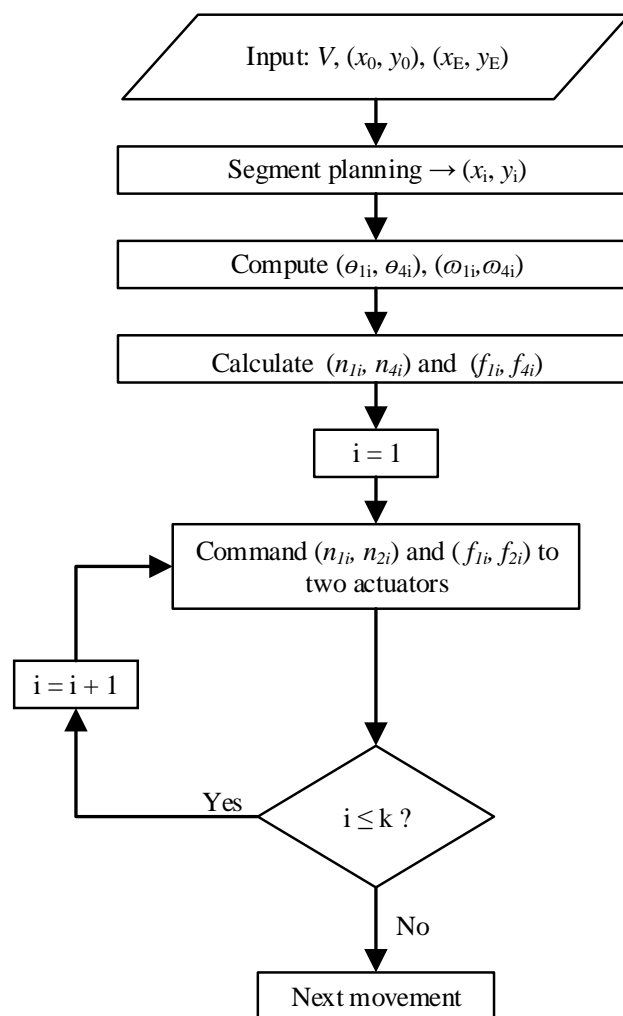


Figure 14. Interpolative algorithm flowchart

Interpolative algorithm is carried out by splitting a straight line or a circular arc into a group of equal tiny segments, from which a collection of interpolative points (x_i, y_i) is achieved. Together

with a desired velocity V , the pulse trains (n_{1i}, n_{4i}) and pulse frequencies (f_{1i}, f_{4i}) are calculated and then provided to the two motors. The flowchart in Fig. 14 demonstrates the linear implementation process that is supported by a supportive command 'ps400_const_move()' in which a pair of two consecutive interpolative points is used as input parameters in sequence from the first point to the last point.

6.2 Graphical user interface

In this 2-DOF parallel robot, the PISO PS400 Card together with the computer forms a PC-based controller. Therefore, a graphical user interface (GUI) in C# is developed for this system as shown in Fig. 15.

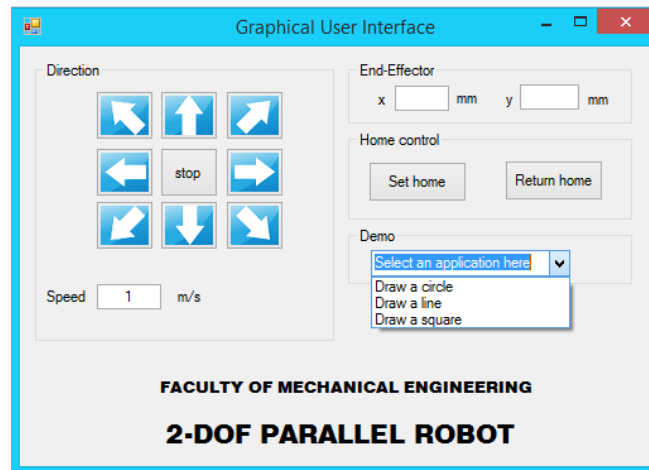
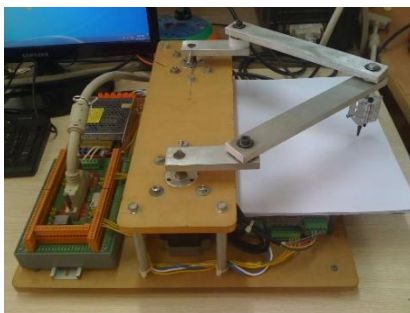


Figure 15. The graphical user interface

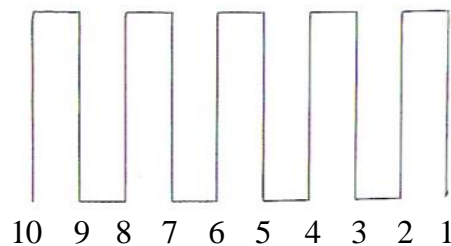
This GUI includes three main groups:

- Information: providing the current position of the end-effector.
- Basic functions: including set home, return home and eight direction buttons
- Demo: drawing circle, line and square.

6.3 Accuracy Evaluation



a) Prototype of 2-DOF parallel robot



b) 10 parallel lines

Figure 16. Prototype and its accuracy validation

A prototype of 2-DOF parallel robot has been implemented as shown in Fig. 16a. To validate its

accuracy, by using “draw a line” function from a starting point, 10 parallel lines having the same length of 40 mm are plotted on a paper sheet as shown in Fig. 16b. Each line is spaced 10 mm apart. These plotting lines are scanned into computer. Experimental results in Table 4 show that the standard deviation of the end-effector is approximate 0.264 mm.

Table 4. Experimental results

Line number	Length (l_i) (mm)
1	39.75
2	39.90
3	40.05
4	40.30
5	40.40
6	40.45
7	40.40
8	40.45
9	40.45
10	40.60
Average	$\bar{l} = 40.275$

The standard deviation is:

$$\sigma_l = \sqrt{\frac{1}{10} \sum_{i=1}^{10} (l_i - \bar{l})^2} = 0.264$$

7. CONCLUSIONS

The paper studied and developed a parallel robot based on 5-bar linkage. There are five types of workspace and three types of singularity existing in this mechanism. Four design criteria have been addressed to simplify the structure design as well as to eliminate the type II singularity zones within the workspace. A prototype of 2-DOF parallel robot has been implemented. From the experiments, the accuracy of the system have been validated approximately ± 0.264 mm. These results are bases for building more complicated applications.

Acknowledgement: The authors would like to thank the Faculty of Mechanical Engineering at Ho Chi Minh City University of Technology for sponsoring this research program.

REFERENCES

- [1]. T.S. Dinh Le and C.B. Pham, *Study, Design and Implement Belt-Driven 2-D CNC Systems*, Proceeding of The 2013 International Symposium on mechatronics and Robotics, December 10-11, 2013, Ho Chi Minh City University of Technology, Viet Nam, pp. 145-149.
- [2]. C. Gosselin and J. Angeles, *Singularity Analysis of Closed-Loop Kinematic Chains*, IEEE Transactions on robotics and automation, Vol. 6, No. 3, June 1990.
- [3]. Figielski, I. A. Bonev and P. Bigras, *Towards Development of a 2-DOF Planar Parallel Robot with Optimal Workspace Use*, IEEE International Conference on Systems, Man and Cybernetics, 2007.